Journal of Computational Electronics 4: 67–70, 2005

Wigner Function-Based Simulation of Quantum Transport in Scaled DG-MOSFETs Using a Monte Carlo Method

ANDREAS GEHRING AND HANS KOSINA
Institute for Microelectronics, TU Vienna, Gußhausstraße 27–29, A-1040 Vienna, Austria
gehring@iue.tuwien.ac.at
kosina@iue.tuwien.ac.at

Abstract. Source-to-drain tunneling in deca-nanometer double-gate MOSFETs is studied using a Monte Carlo solver for the Wigner transport equation. This approach allows the effect of scattering to be included. The subband structure is calculated by means of post-processing results from the device simulator Minimos-NT, and the contribution of the lowest subband is determined by the quantum transport simulation. By separating the potential profile into a smooth classical component and a rapidly varying quantum component the numerical stability of the Monte Carlo method is improved. The results clearly show an increasing tunneling component of the drain current with decreasing gate length. For longer gate lengths the semi-classical result is approached.

Keywords: device simulation, quantum transport, Wigner equation, double-gate MOSFET

1. Introduction

Double-gate (DG) MOS transistor structures have been proposed to improve the performance of scaled logic devices and to overcome some of the most severe problems encountered in the further down-scaling of bulk MOS field-effect transistors [1]. However, with channel lengths below 25 nm, the question of the importance of quantum effects in the lateral direction, such as source-to-drain tunneling, arises. Frequently, ballistic transport is assumed which allows the device to be simulated using pure quantum-mechanical approaches [2, 3]. However, with carrier mean free paths in the range of few nanometers [4], scattering-limited transport may still be dominant. The effect of scattering has been assessed using classical Monte Carlo methods including a quantum correction [5] or the scattering rates of the two-dimensional electron gas [6]. A rigorous transport model accounting for both, quantum interference phenomena and scattering mechanisms, is based on the Wigner equation including a suitable collision operator.

This equation can be solved using recently developed Monte Carlo methods [7,8]. This work reports on the enhancement of the Wigner Monte Carlo simulator described in [8] for the simulation of silicon-based devices. The algorithm for annihilation of numerical particles now takes into account the multi-valley band structure of silicon. Particular emphasis is put on the separation of the potential profile into a smooth classical component and a rapidly varying quantum component.

2. Transport Model

The potential operator of the one-dimensional Wigner equation is given by the following convolution integral,

$$\Theta_w[f_w](k,x,t) = \int_{-\infty}^{\infty} V_w(q,x) f_w(k-q,x,t)\,\mathrm{d}q, \tag{1}$$

where V_w denotes the Wigner potential.

$$V_w(q,x) = \frac{1}{2\pi i\hbar} \times \int_{-\infty}^{\infty} \left(V\left(x+\frac{s}{2}\right) - V\left(x-\frac{s}{2}\right)\right) \mathrm{e}^{-iq\cdot s}\,\mathrm{d}s \tag{2}$$

The potential energy of electrons is denoted by $V(x)$. This energy is assumed to be constant outside the simulation domain. When a voltage is applied to the device, the integrand of (2) does not vanish for large s, $V(x+s/2)-V(x-s/2)\to(-e)V_{\text{app}}$, and hence the Fourier integral diverges at $q=0$. This gives rise to a singularity in $V_w(q,x)$. For this reason, we introduce some small wave number, q_c, and exclude the interval $|q|<q_c/2$ from the domain of integration in (1).

The integral over the small wave numbers is treated separately. The linearization $f_w(k-q)\simeq -q\,\partial_k f_w(k)$ then leads to a local classical force term.

$$\Theta_{cl}[f](k,x,t)=\frac{1}{\hbar}\frac{\partial V_{\text{cl}}(x)}{\partial x}\frac{\partial f_w(k,x,t)}{\partial k} \tag{3}$$

$$V_{cl}(x)=\frac{1}{2\pi}\int_{-q_c}^{q_c}\hat{V}(q)\mathrm{e}^{iqx}\mathrm{d}q \tag{4}$$

In this equation, $\hat{V}(q)$ is the Fourier transform of the potential. Note that (4) is defining an ideal low pass filter with cut-off wavenumber q_c. Therefore, we consider a spectral decomposition of the potential profile into a slowly varying, classical component (4) and a rapidly varying, quantum mechanical component.

$$V(x)=V_{cl}(x)+V_{qm}(x) \tag{5}$$

An example for this decomposition is shown in Fig. 1 for the subband energy of a 10 nm gate length device as described in Section 3.

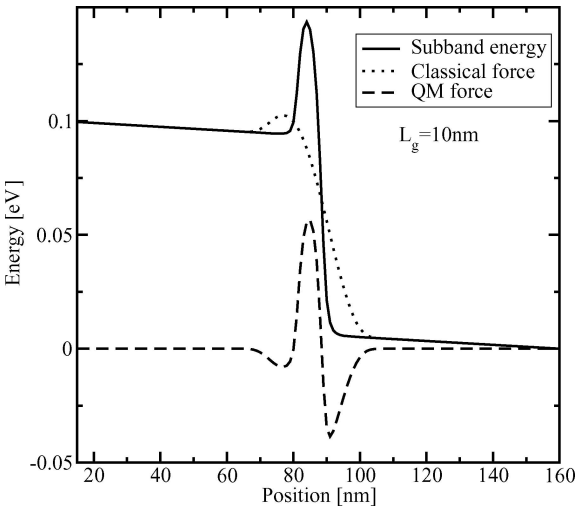

Figure 1. Potential decomposition of the subband potential into a classical part $V_{cl}(x)$ and a quantum-mechanical part $V_{qm}(x)$ for the 10 nm gate length device.

This decomposition yields a Wigner equation including both, a local classical force term with $F_{\text{cl}}=-\partial_x V_{\text{cl}}$ and a nonlocal potential operator.

$$\left(\frac{\partial}{\partial t}+v_x\frac{\partial}{\partial x}+\frac{F_{\text{cl}}}{\hbar}\frac{\partial}{\partial k}\right)f_w(k,x,t)=\left(\frac{\partial f_w}{\partial t}\right)_{\text{coll}}+\int V_w^{\text{qm}}(q,x)f_w(k-q,x,t)\,\mathrm{d}q \tag{6}$$

Scattering is taken into account through the Boltzmann collision operator. The Wigner potential is calculated from the quantum mechanical potential component, V_{qm}.

$$V_w^{qm}(q,x)=\frac{1}{2\pi i\hbar}\times\int_{-\infty}^{\infty}\left(V_{qm}\left(x+\frac{s}{2}\right)-V_{qm}\left(x-\frac{s}{2}\right)\right)\mathrm{e}^{-iq\cdot s}\,\mathrm{d}s \tag{7}$$

The devices considered in this work consist of a quantum region that is embedded in an extended classical region. In the quantum region a uniform grid with step size Δx is assumed. The number of points for the discrete Fourier transform is N_k. A fairly large value for N_k in the range 10^2–10^3 is chosen in order to obtain a good resolution of the Wigner potential. In this case the domain of the Fourier transform, $L_{\text{FT}}=N_k\Delta x$, will be much larger than the quantum region. Therefore, for the purpose of the Fourier transform the potential outside the quantum region is extrapolated by a constant. In the discrete system, the classical potential defined by (4) becomes:

$$V_{cl}(x_j)=\frac{\sum_l w_{jl}\,V(x_l)}{\sum_l w_{jl}},\quad -\frac{N_k}{2}\le l\le\frac{N_k}{2} \tag{8}$$

$$w_{jl}=\frac{\sin((j-l)q_c\Delta x)}{(j-l)q_c\Delta x} \tag{9}$$

In the simulator the value of the cut-off wavenumber q_c is specified by a cut-off wave length as

$$q_c=\frac{2\pi}{\lambda_c} \tag{10}$$

It can be seen from (9) that $\lambda_c=2\Delta x$ would give $V_{cl}(x_j)=V(x_j)$ and hence the quantum component would vanish. This choice of λ_c apparently gives the classical limit of the discrete system. For a quantum transport calculation one has to choose $\lambda_c\gg 2\Delta x$. In this work we assume $\lambda_c=30\,\text{nm}$.

3. Results and Discussion

As test devices for the above described Monte Carlo method we use double-gate MOSFETs with gate lengths of 60, 25, 15, and 10 nm and silicon film thicknesses of 20, 10, 5, and 3 nm, respectively. For simplicity, metal gates with midgap work function have been assumed. A source/drain doping of 5×10^{19} cm^{-3} with abrupt doping profile and undoped channel was chosen, as shown for the 25 nm device in Fig. 2. To obtain a potential profile for the quantum transport simulation a classical simulation using Minimos-NT [9] has been performed.

To account for the effect of confinement due to the small silicon film thickness, the first longitudinal subband ($m_l = 0.91m_0$) was calculated in a post-processing step from the Schrödinger equation.

$$\left(-\frac{\hbar^2}{2m_l}\frac{\mathrm{d}^2}{\mathrm{d}y^2} + V(x, y) \right) \Psi(y) = \mathcal{E}_x \Psi(y) \quad (11)$$

Due to the computational requirements of the quantum Monte Carlo simulation the potential is not determined self-consistently with the quantum mechanical problem in this study. All simulations take phonon scattering into account. As a first order approximation a semi-classical scattering model with bulk scattering rates is used. Effects due to finite interaction time such as the inter-collisional field effect and collisional broadening are hence neglected. Figure 3 shows the resulting subband edges along the channel of the different devices at a drain bias of 0.1 V. Due to the different silicon thicknesses, the subband energies increase with decreasing gate length. The decomposition procedure described above is applied to obtain a classical and a quantum-mechanical force term.

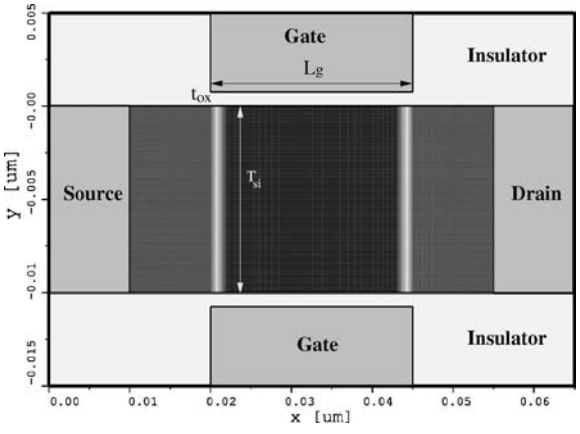

Figure 2. Sketch of the 25 nm gate length double-gate MOSFET structure simulated by Minimos-NT.

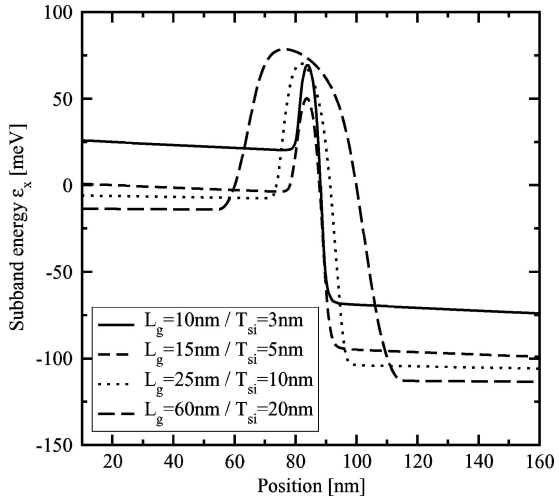

Figure 3. First longitudinal ($m_l = 0.91m_0$) subband for devices with different gate lengths and silicon thicknesses at a source-drain bias of 0.1 V.

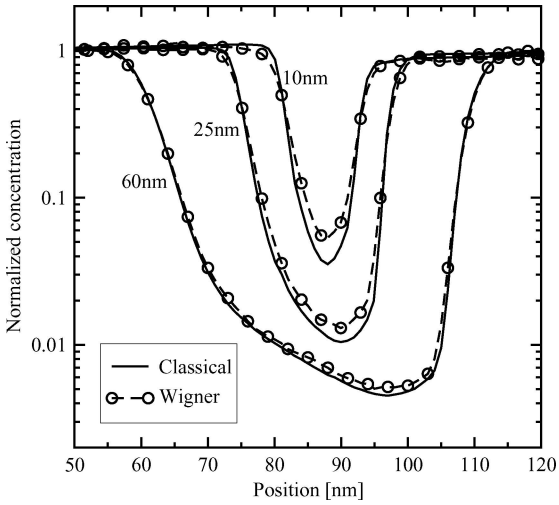

Figure 4. The carrier concentrations in the 10 nm, the 25 nm, and the 60 nm gate length devices at 0.6 V drain bias for the classical and the Wigner Monte Carlo simulations.

The carrier concentrations in the different devices at a drain bias of 0.6 V resulting from the quantum Monte Carlo simulation are shown in Fig. 4. The difference is significant for the 10 nm gate length device, for which the Wigner simulation predicts carrier concentrations in the channel almost 50% higher than predicted by the classical simulation.

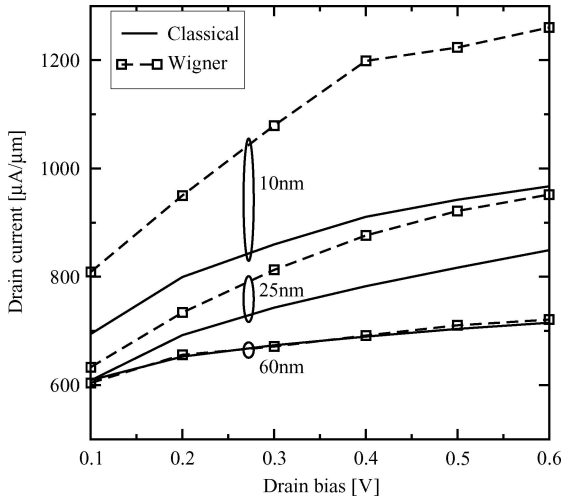

Figure 5. Output characteristics of the 10 nm, the 25 nm, and the 60 nm gate length devices using classical and Wigner Monte Carlo. The source-to-drain tunneling current component is clearly visible for the short-channel devices.

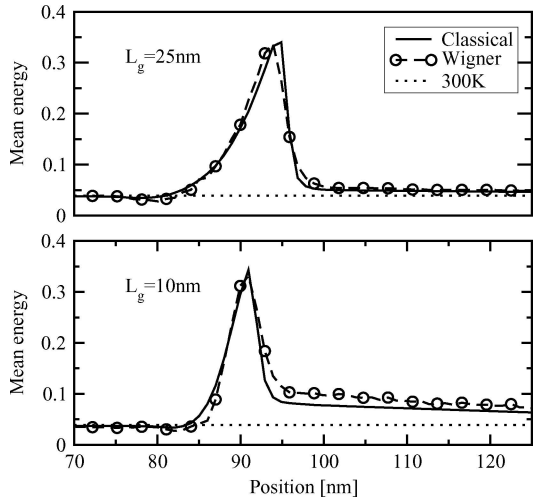

Figure 6. The mean particle energy in the 10 nm, the 25 nm, and the 60 nm gate length device at 0.6 V drain bias for the classical and the Wigner Monte Carlo simulations.

The output characteristics are shown in Fig. 5. At 60 nm, the Wigner calculations reproduce the classical results, while they predict higher currents at smaller gate lengths. This can be attributed to source-drain tunneling, which is not present in the classical simulation.

The resulting mean energy of the 25 and 10 nm gate length devices are shown in Fig. 6 for a drain bias of 0.6 V. The difference between the classical and Wigner simulation results is very small. For the 10 nm device, due to the high electric field in the channel, the carriers cool down only slowly and are not fully thermalized at the drain end of the channel.

4. Conclusions

The Wigner Monte Carlo method allows for a direct comparison of semi-classical and quantum transport results. A spectral decomposition of the potential profile into rapidly varying and a smoothly varying components is proposed. Treating the latter as a classical force removes the singularity of the Wigner potential at $q = 0$. This measure improves the robustness of the numerical method. Double-gate MOSFETs of different gate lengths have been studied. The edge of the lowest subband are calculated using Minimos-NT. The Wigner transport calculation reproduces the semi-classical result for the long channel device and predicts a significant source-to-drain tunneling component in the drain current at very short gate lengths.

Acknowledgment

This work has been partly supported by the Austrian Science Fund FWF, project P17285-N02, and the European Commission, project NESTOR, IST-2001-37114. Discussions with Christian Ringhofer are acknowledged.

References

1. J.-P. Colinge, "Multiple-Gate SOI MOSFETs," *Solid-State Electron.*, **48**, 897 (2004).
2. M. Lundstrom and Z. Ren, "Essential physics of carrier transport in nanoscale MOSFETs," *IEEE Trans. Electron Devices*, **49**(1), 133 (2002).
3. R. Venugopal et al., "Simulation of quantum transport in nanoscale transistors: Real versus mode-space approach," *J. Appl. Phys.*, **92**(7), 3730 (2002).
4. C. Jungemann et al., "Investigation of strained Si/SiGe devices By MC simulation," *Solid-State Electron.*, **48**, 1417 (2004).
5. G.A. Khatawala et al., "Monte carlo simulations of double-gate MOSFETs," *IEEE Trans. Electron Devices*, **50**(12), 2467 (2003).
6. F. Gámiz et al., "Double gate silicon on insulator transistors. A Monte Carlo study," *Solid-State Electron.*, **48**, 937 (2004).
7. L. Shifren et al., "A wigner function-based quantum ensemble Monte Carlo study of a resonant tunneling diode," *IEEE Trans. Electron Devices*, **50**(3), 769 (2003).
8. H. Kosina et al., "A Monte Carlo method seamlessly linking quantum and classical transport calculations," *J. Computational Electronics*, **2**(2–4), 147 (2002).
9. Institut für Mikroelektronik Technische Universität Wien, Austria, *MINIMOS-NT 2.1 User's Guide* (2004).